THERMAL PERFORMANCE MODELING AND MEASUREMENTS OF LOCALIZED WATER COOLED COLD PLATE

Seaho Song, Kevin P. Moran, Donald P. Rearick
Enterprise Systems
IBM Corporation
Poughkeepsie, NY

and

Seri Lee
Aavid Engineering, Inc.
Laconia, NH

ABSTR4CT

Two different water-cooled cold plate designs to handle highly localized heat dissipations in electronic packaging applications are introduced. One design employs drilled holes as the flow conduit, and the other uses a specially formed copper tube. These designs offer high thermal performance at low water flow and pressure drop requirements. Measurements and models for thermal and hydraulic performance are presented. The model predictions and the measurements are in excellent agreement.

I. INTRODUCTION

As the electronics industry continues to face the increasing trend of heat dissipation in electronic components, water cooling is fast becoming an attractive design option for high performance thermal management. In designing a water-cooled cold plate the followings are some of the important design parameters:

o thermal performance
0 water flow rate
0 pressure drop
0 mechanical strength
0 corrosion & fouling
0 manufacturability
0 cost

Water flow rate and pressure drop influence the size of pumping and plumbing requirements, and ultimately the cost and the physical volume of coolant distribution system. Therefore in designing cold plates, it is of great importance to minimize the water flow rates and the pressure drop, yet ensuring sufficient thermal performance.

In dense electronic packaging applications, there may be a few high heatdissipating components which require a cold plate with a very high level of cooling performance. Certain components with odd physical shapes, such as transformers, may present the cold plate designer with the challenge of providing water passages to restricted areas. Figure 1 shows the cooling requirements for a cold plate

used with a high-heat dissipating power supply. Each of the six shaded areas (shown as four areas, A, B, C & D) in the figure must COOl a heat dissipation rate of 5 to 15 watts per square centimeter. Also shown in the figure are areas (designated as 'open area') where water passage is not allowed due to other packaging requirements. The combination of requirements for highly localized performance and restricted flow passage adds additional challenge to the cold plate design for this application.
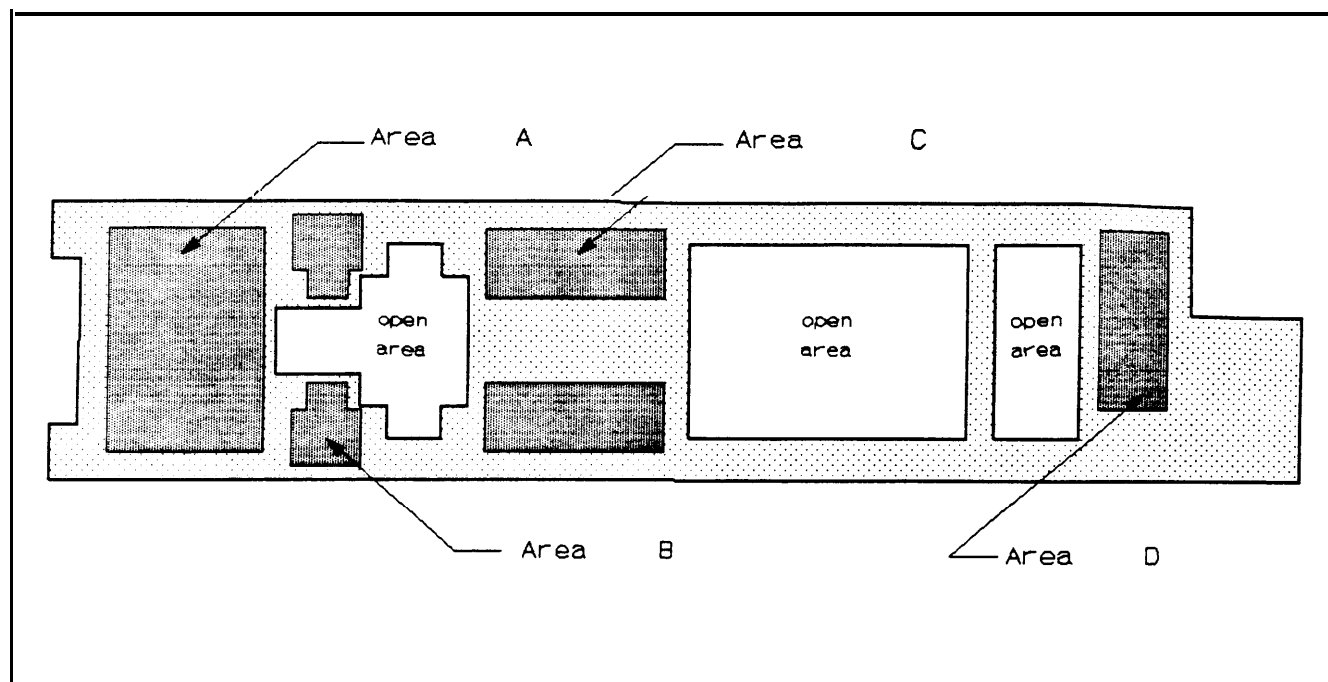

Figure 1: Typical Cooling Requirements

In this paper, two rather unique cold plate design concepts are presented to address the requirements outlined in Figure 1. They are:

o drilled hole design
o press-fit tube design

The cross sections for the designs are shown in Figure 2. These two concepts are suitable to accommodate requirements for localized high-cooling performance, and allow water passages to be laid out around the geometric restrictions.

Developments of the cold plates using these concepts to meet the requirements shown in Figure 1 are presented in this paper. Prototype cold plates have been built, and measurements were made for thermal performance and pressure drop. Models were developed to predict the thermal performance and the pressure drop. Comparisons between the predicted and the measured values over a range of water flow rate are presented.

II. COLD PLATE DESIGN AND MANUFACTURABILITY

When using water for the cooling medium special care must be given to the selection of materials in order to prevent corrosion and the buildup of fouling deposits. Copper was chosen as the material for

the water passages for its excellent thermal characteristics and corrosion resistance.

Figure 3 shows an isometric view of the drilled hole cold plate design and a schematic of the water flow. Note that the small cooling holes are locally concentrated under areas A, B, C, and D. The cold plate was designed to make use of cost effective manufacturing processes while still providing high efficiency cooling. A copper plate is machined to the required outline shape. Multiple small holes are then drilled below the outside heat transfer surface areas (Figure 1). The size and number of holes can be varied to meet the heat flux and flow requirements. Large holes are then drilled to interconnect the small holes and to serve as main water ducts. A process called gun-drilling is used to drill the very long holes. Care must be taken to prevent internal burrs that would restrict flow through the small holes. The holes are then closed along the cold plate edges by brazing or electron-beam welding plugs in place. The outside surface of the cold plate is nickel plated to prevent oxidation.
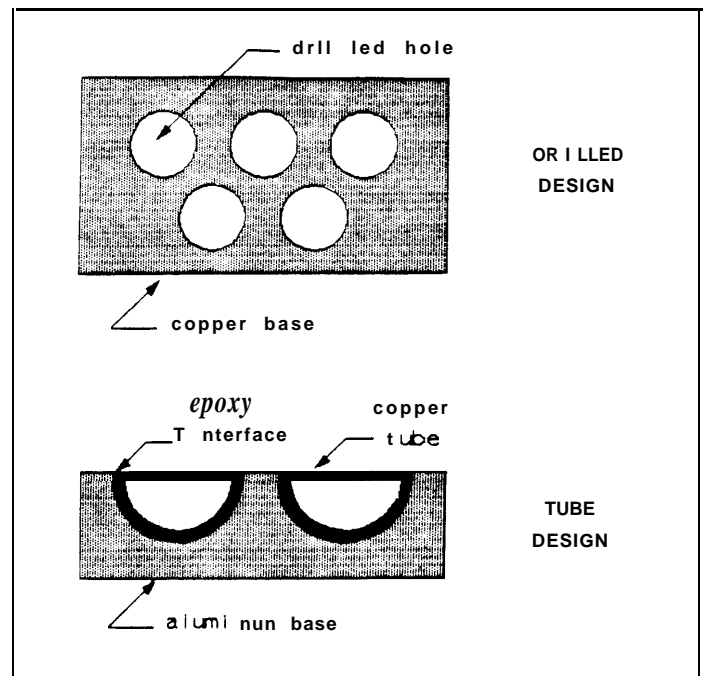

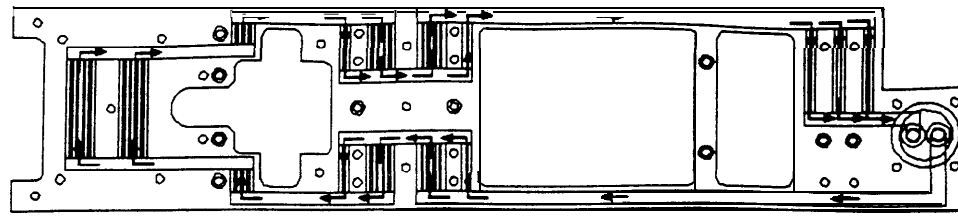**Figure** 2: Cold Plate Cross Sections

A disadvantage of this approach maybe that copper, although it has excellent thermal properties, adds a significant amount of weight to the assembly. Also the cost is relatively high due to the special operations required for brazing or electron-beam welding.

An isometric view of press-fit tube design (referred to as the tube design hereafter) is shown in Figure 4. This two piece cold plate technology is patent pending by, and the corresponding assembly process is proprietary to Aavid Engineering, Inc. The cold plate is constructed with a copper tube pressed into grooves machined in an aluminum base plate. By confining the water flow to within the copper tube, this design allows the base plate to be constructed of aluminum, thereby reducing the weight and cost of the assembly. The tube is formed to a serpentine pattern to provide highly localized cooling capabilities at heat dissipating areas. A thermal epoxy is used to provide the thermal interface between the tube and the base plate.

III. THERMAL AND PRESSURE MEASUREMENTS

Prototype cold plates were built for both the drilled and the tube designs to obtain thermal performance and pressure drop measurements. Thermal performance for each local cooling area (areas A, B, C and D in Figure 1) was characterized by thermal resistance defined as:

$$R = \frac{\overline{T_{cp}} - T_M}{Q} \tag{1}$$

71

FLOW SCHEMATIC

HOLE PLUGS

SMALL HOLES
IN THERMAL
TRANSFER AREA
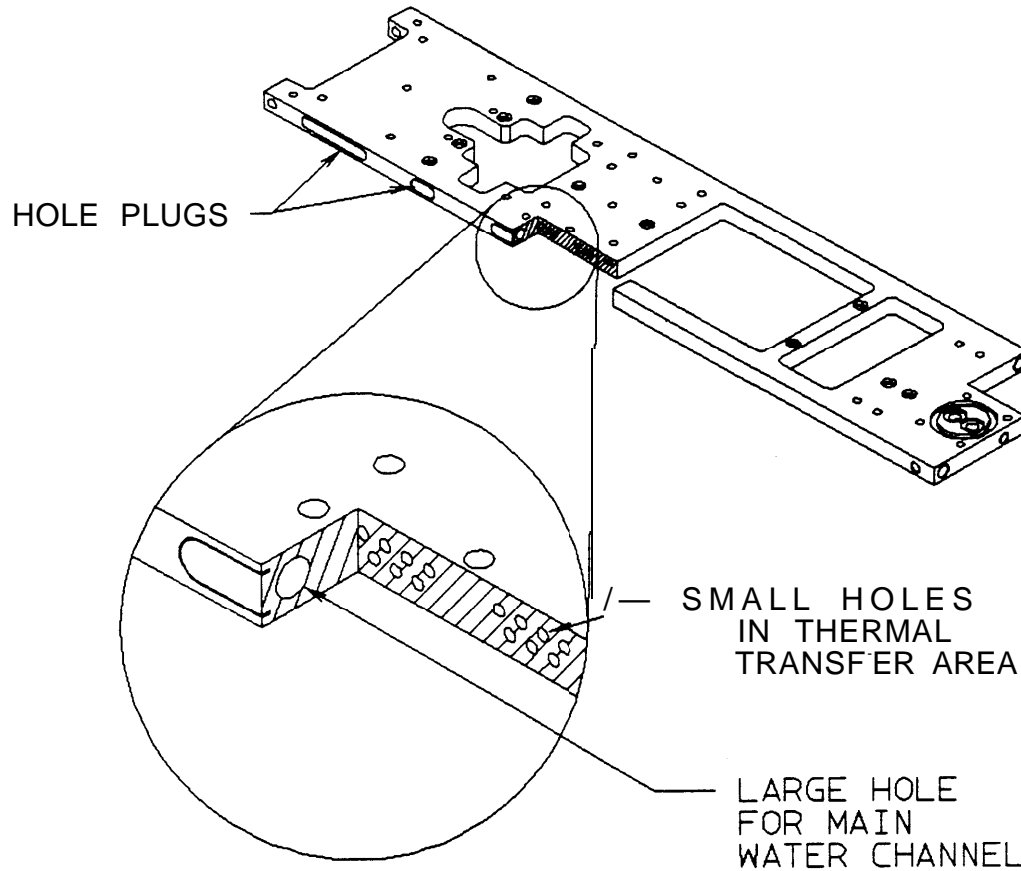
LARGE HOLE
FOR MAIN
WATER CHANNEL

Figure 3: Drilled Design Cold Plate

where T_{cp}, $T_{inlet\ water}$, Q are the average cold plate temperature over a local area, local inlet water temperature, and local heat flow rate, respectively.

Cold plate temperature measurements were made using 'T-type' thermocouples epoxy-glued directly on the cold plate surface. Two to five thermocouples were placed on each local cooling area, and the readings from the thermocouples were averaged to yield the local mean temperature.

To provide heat input, heater blocks were madefromoxygen-free copper to the same footprints
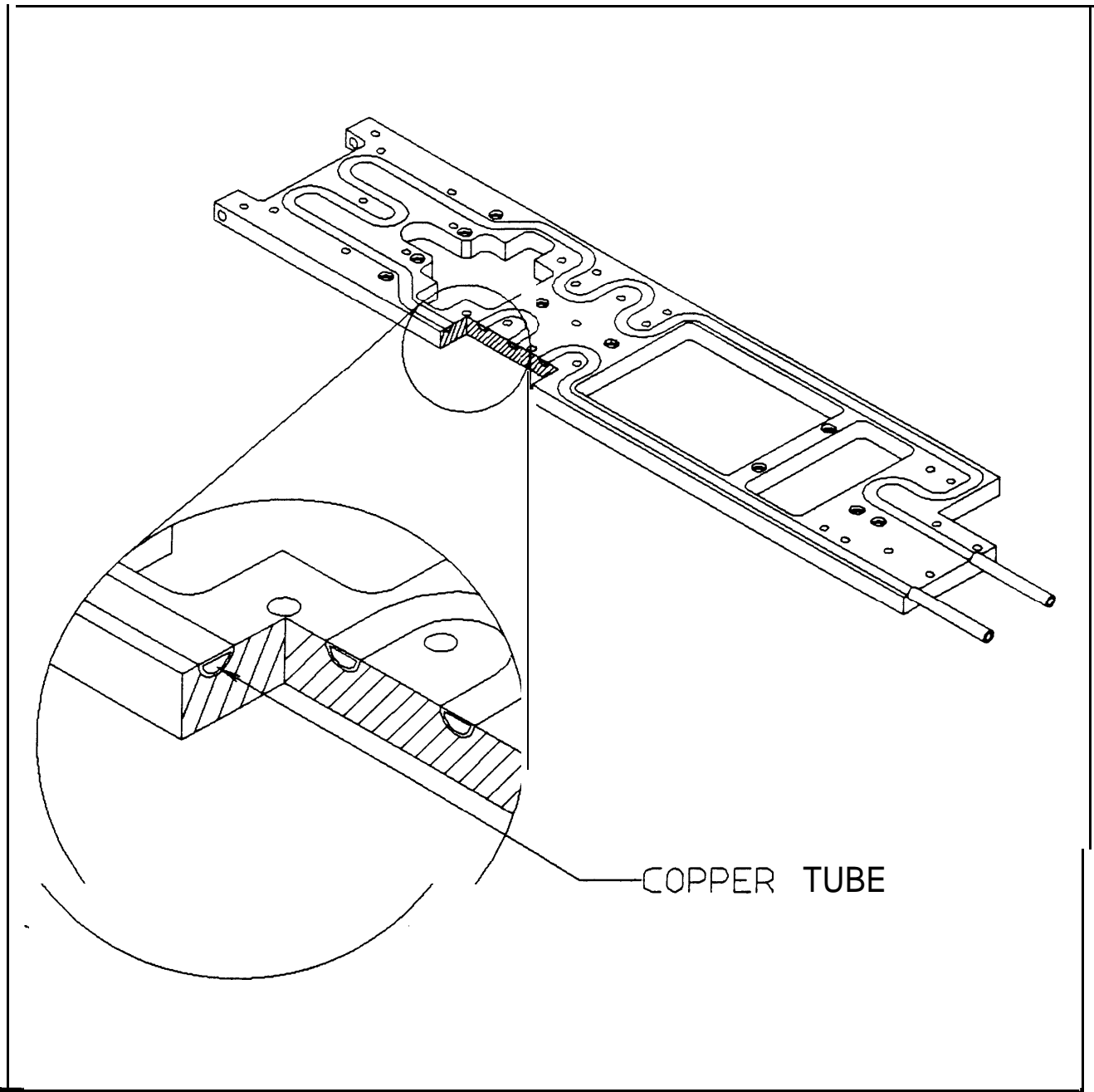
Figure 4: Press-Fit Tube Design Cold Plate

of cold plate cooling areas. Holes were drilled in the heater blocks, and pencil-type heaters with thermally conducting paste were inserted. The electrical current through and the voltage drop across the heaters were monitored to estimate the power input. Rectangular grooves were machined on the bottom surface (Figure 5) to clear thermocouple wires and beads.

For the heat transfer measurements, the heater blocks were mounted directly on the cold plate using thermally conducting paste applied in the interfaces. For each test, the heat input was provided to only one area of a cold plate at a time by applying the electrical power to the heaters in the corresponding block. Thermal measurements for each area of both cold plate designs were obtained for

the water flow rate range of 0.5 to 1.5 GPM. The temperature and heat input measurements for each area and flow rate were then converted to the thermal resistance according to Equation 1. In order to compare the cooling effectiveness, the obtained thermal resistances were in turn converted to an effective heat transfer coefficients defined as:

$$h_{eff} = \frac{1}{R A} \qquad (2)$$

where A is the area of local cooling surface (Figure 5).

Figure 5: Thermal Performance Test Setup

IV. PERFORMANCE MODELING AND COMPARISON WITH MEASUREMENTS

In this section, analytical modeling procedures are described for predicting the total pressure drop and thermal performance of both the tube and the drilled cold plates. Whenever possible, simple existing correlation equations that are readily available in common handbooks were used. It will be shown, later in this section, through comparisons with the present measurements that such correlations are sufficient and accurate for engineering predictions.

Pressure Drop

The total pressure drop Δp of a given system can be found from

$$\frac{\Delta p}{\rho u_m^2/2} = f \frac{A_{wet}}{A_c} + \sum K \qquad (3)$$

where U_m is the bulk mean velocity, f is *the* fanning fiction factor, defined as the ratio of the wall shear *stress* τ_w to the flow kinetic energy per unit volume, $\rho u_m^2/2$:

$$f = \frac{\tau_w}{\rho u_m^2/2} \qquad (4)$$

A_{wet} and A_c are the wetted surface area and the cross sectional area of the duct, respectively, and K is the local resistance coefficient accounting for the pressure losses due to factors other than the surface shear fiction, such as entrances, exits and turns, etc.

Since the range of water flow examined in the present investigation spans over the transient through turbulent flow regimes, it is necessary to employ a comprehensive correlation equation covering these regimes. Churchill [1977] proposed one such correlation for computing the fanning fiction factor over the entire flow regimes from laminar to turbulent flows:
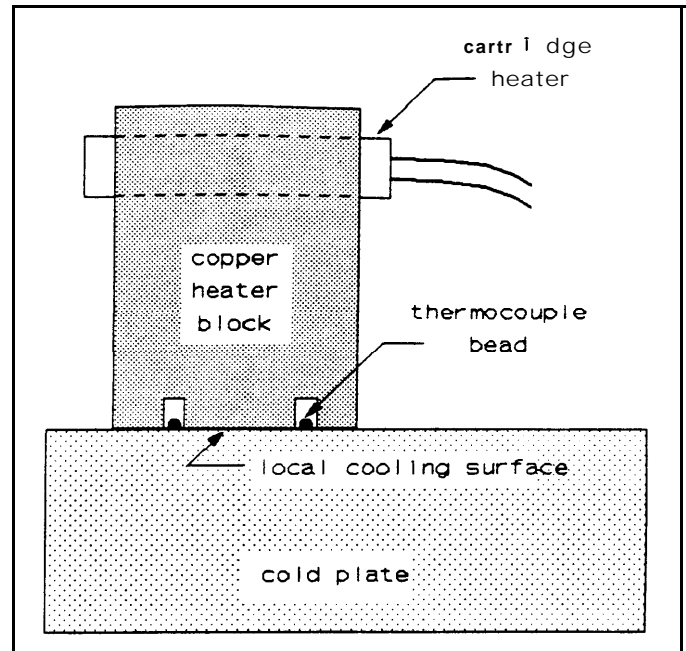
$$\frac{2}{f} = \left\{ \frac{1}{[(8/Re)^{10} + (Re/36500)^{20}]^{1/2}} + [2.21 \ \ln(Re/7)]^{10} \right\}^{1/5} \tag{5}$$

where the Reynolds number Re is defined based on the hydraulic diameter D_h:

$$Re = \frac{u_m D_h}{v} \tag{6}$$

It is to be noted that the above correlation, Eq.(5), is constructed for **fully** developed flows. For larninar *(Re < 2100)* and turbulent *(Re > 4000)* flows, it is in excellent agreement with other available data and, for transition flow (2100 **< Re < 4000),** it is found to be in fair to good agreement with existing experimental results [Kakac et al., 1987].

For estimation of the local pressure losses around smooth turns of a
circular tube, the following expression can be used [Idelchik, 1986]:

$$K = K_a \ K_b \tag{7}$$

with K_a and K_b obtained from:

$$K_a = \begin{cases} 0.9 \ sin \ a & \textit{if } a \le 70° \\ 1.0 & \textit{if } a = 90° \\ 0.7 + 0.35 \ \dfrac{\alpha}{90°} & \textit{if } a \ge 100° \end{cases} \tag{8}$$

$$K_b = \begin{cases} \dfrac{0.21}{\Upsilon^{1/4}} & \textit{if } 0.5 \ \le y \le \ 1.0 \\ \dfrac{0.21}{\sqrt{\gamma}} & \textit{if } \gamma > 1.0 \end{cases} \tag{9}$$

In the above expressions, *a* is the turning angle and y is the dimensionless turning radius given by

$$\gamma = \frac{r_0}{D} \tag{10}$$

where *r.* and *D* are the center-line turning radius and inside diameter of the circular tube, respectively.

Using the expressions presented above, the total pressure drops are computed for both the tube and the drilled designs as a **function** of volumetric flow rate, and the results are compared with the present measurements in Figure 6. The property values of water were obtained at the inlet temperature of *22°C* and were assumed to be constant throughout the present computation.

For the tube design case, the hydraulic diameter and the cross sectional area were found to be *4mm* and 17.6mrn, respectively, and the total tube length of *1.29m* was used in the computation. In

addition, the resistance coefficients at various turns are calculated using Eqs.(7) through (10), and it is found that the total resistance coefficient involving four-45°, six-90°, and ten-1800 turns in the system is approximately equal to 3.65.

For the drilled design case, Eq.(3) is used for each region of different flow cross sectional area. The fanning fiction factor was computed based on the hole or hydraulic diameter, average flow velocity and average flow length of each tube section. In addition to the pressure drop due to the skin friction, the entrance and exit losses were needed to be computed as the flow enters and exits each section. An estimated resistance coefficient value of 1.5 was used uniformly for *each* section to account for these losses combined with the losses incurred by the sharp perpendicular turns at the entrance and exit of each section. The sectional pressure drops are then summed to represent the total pressure drop across the entire cold plate. As can be seen from Figure 6, the agreement between the predictions obtained by using the above correlations and the measurements, represented by discrete symbols, are excellent for both the tube and drilled designs.

Heat Transfer

To determine analytically the effective heat transfer coefficient h_{eff} as defined by Eq.(2), it is necessary to identify the thermal path and determine the thermal resistance attributed by each component within the path. These include material resistances of the cold plate matrix and the tube wall as well as the interracial resistance across the thermal epoxy layer, and the convective heat transfer within the ducts. In the following, detailed procedures for obtaining these component resistances is described starting with the determination of the convective heat transfer coefficient or the convective resistance in duct flows.

Similar to the correlation used in estimating the pressure drop, the following correlation developed also by Churchill [1977] for $O < Pr < \infty$ and $Re \leq 10^6$, spanning laminar, transient, and turbulent flow regimes, was employed for calculating mean Nusselt numbers for filly developed flows, Nu_∞, in ducts:

$$Nu_\infty^{10} = Nu_l^{10} + \left\{ \frac{\exp[(2200 - Re)/365]}{Nu_l^2} + \frac{1}{Nu_t^2} \right\}^{'s} \tag{11}$$

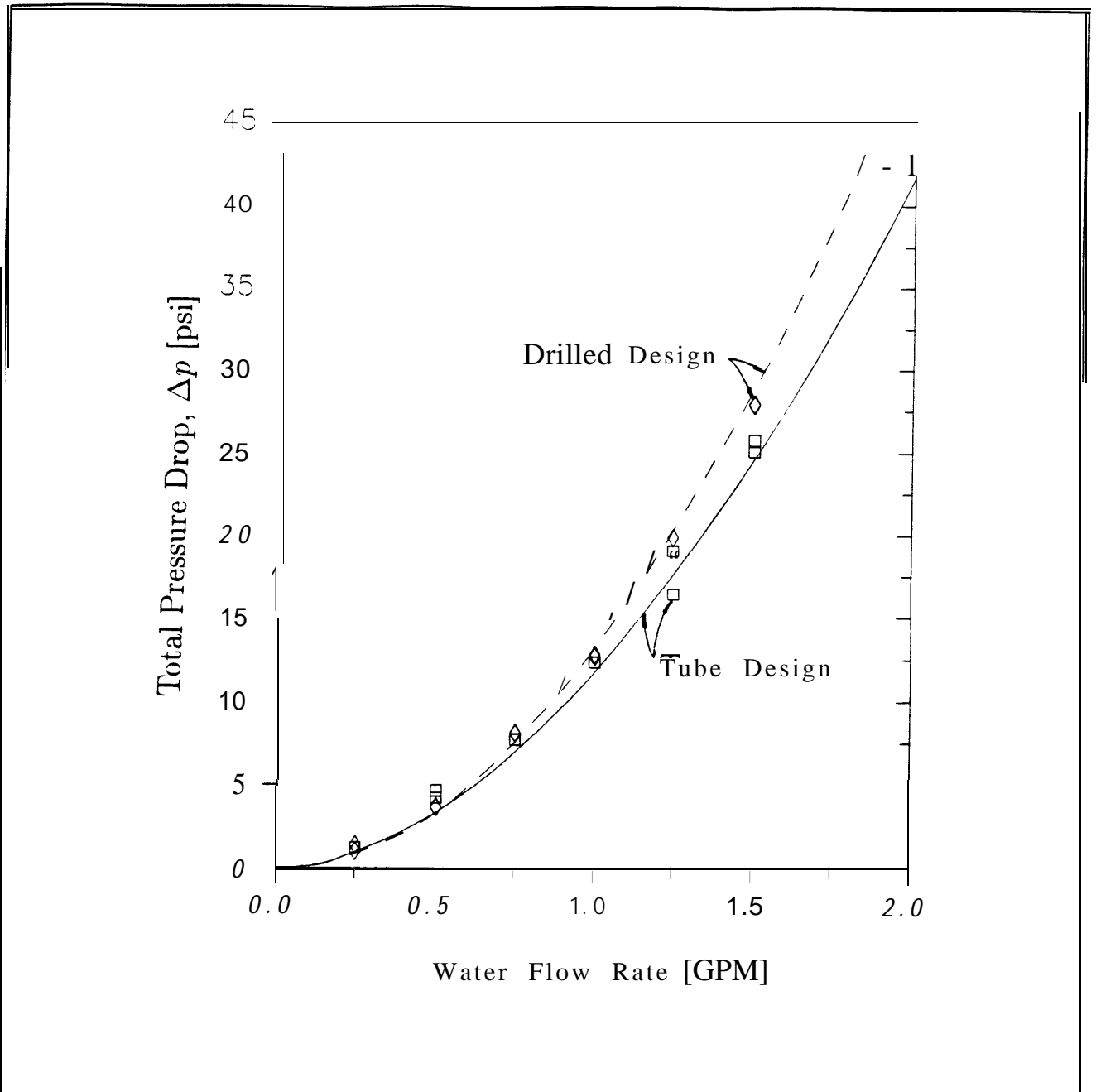where, assuming an isothermal boundary condition for conservative estimates of the Nusselt numbers,

$$Nu_l = 3.66 \tag{12}$$

$$Nu_t = 4.8 + \frac{0.079 \ (f/2)^{1/2} \ Re \ Pr}{(1 + Pr^{4/5})^{5/6}} \tag{13}$$

Here, Nu_l and Nu_t denote the laminar and turbulent components within the above blending equation, and f is obtained from Eq.(5).

For thermally developing flows, a modified correlation was developed bY Al-Arabi [1982] as

Figure 6: Comparison of Total Pressure Drop versus Water Flow Rate for Tube and Drilled Cold Plates

$$\frac{Nu_m}{Nu_\infty} = 1 + \frac{0.68 + 3000/Re^{0.81}}{(L/D_h)^{0.9} Pr^{1/6}} \tag{14}$$

where Nu_∞ stands for the filly developed Nusselt number obtained from Eq.(1 1) and L is the duct length. This correlation is valid for $L/D_h > 3$, $3500 < Re < 10^5$ and $0.7 < Pr < 75$. The above Nusselt number is defined using the hydraulic diameter as the length scale:

$$N u_m \equiv \frac{h_m D_h}{v} \tag{15}$$

Upon obtaining the average heat transfer coefficient h_m, the convective resistance can be calculated from

$$R_h = \frac{1}{h_m A_{wet}} \tag{16}$$

where A_{wet} is the heat transfer area of the duct.

With this convective resistance, *the* total resistance R from the fluid to the surface of a cold plate was obtained simply by adding other pertinent resistances associated within the thermal path. For the tube design, it becomes

$$R = R_h + R_{tube} + R_{epoxy} + R_{cp} \tag{17}$$

where R_{tube}, R_{epoxy} and R_{cp} represent the thermal resistances of the copper tubing, epoxy layer and aluminum matrix of the cold plate, respectively. They are obtained from

$$R_{tube} = \frac{\ln(r_2/r_1)}{k_{cu} 2\pi L} \tag{18}$$

$$R_{epoxy} = \frac{t}{k_{epoxy}\ 0.65\ (2\pi r_2) L} \tag{19}$$

$$R_{cp} = \frac{r_2/w + \ln(w/2\pi r_2)/4\pi}{k_{al} L} \tag{20}$$

with r, being one half of the hydraulic diameter of the copper tubing, r_2 *is* equal to the sum of *r,* and the tube thickness of 1. 14mm, and w = 19.1mm = 0.75", the distance between the centerlines of copper tubes. The thickness of the epoxy layer, *t,* was taken to be *0.045mm* which is rough] y equal to *the* average of the epoxy layer thicknesses measured under a microscope at various locations around *the* tube. Also, $k_{cu} = 393\ W/mK$, $k_{al} = 209\ W/mK,$ and $k_{epoxy} = 2.7\ W/mK.$

For the drilled design, the total resistance becomes

$$R = R_h + R_{cp} \tag{21}$$

where R_{cp} represents the material resistance of the copper matrix of the cold plate, expressed as either

$$R_{cp} = \frac{\ln(4\delta/D)}{k_{cu} 2\pi L} \tag{22}$$

78

for the large holes *(D = 6mm),* or

$$R_{cp} = \frac{\ln[(2s/\pi D)\sinh(2\pi\,6/s)]}{k_{cu}2\pi L} \tag{23}$$

for the small holes *(D = 2mm).* Here, δ is the depth of the holes measured from the cold plate surface, and s is the pitch distance of *2mm* holes. The expressions for R_{cp}, Eqs. (20), (22) and (23), are either derived or rewritten from the case examples presented in Guyer [1989].

It is to be noted that the heat transfer coefficient used in the definition of the Nusselt numbers appearing above is given in terms of the temperature difference between the tube wall and the mean bulk flow:

$$h_m = \frac{Q/A_w}{T_w - T_m} \tag{24}$$

Therefore, in order to determine the effective heat transfer coefficient, as defined in Eq. (2), one needs to use the following expression, which is developed by balancing the total heat transfer into the fluid with the enthalpy increase in water flow from the inlet to the outlet:

$$h_{e!} = \frac{\dot{m}\,C_P\{1 - \exp[1/(R\,m\,c_p)]\}}{A} \tag{25}$$

where m is the mass flow rate and *R is* from either Eq.(17) for the tube design, or (21) for the drilled design.

The effective heat transfer coefficients were computed as a function of the volumetric flow rate using the above equations. An examination of the predicted results indicated that the flow through the *2mm* holes of the drilled cold plate is going through the transient flow regime when the flow rate is generally less than 1 *GPM,* resulting in much smaller effective heat transfer coefficients as compared to the measured values. However, considering that the flow has to make severe turns as it enters the smaller holes, turbulent assumptions were made for all the flows in the small holes throughout the flow range. This assumption was incorporated herein by simply letting

$$Nu_m = Nu_t \tag{26}$$

to replace Eq.(11) for *2mm* holes with Nu_t given by Eq.(13).

The final results are in excellent agreement with the measurements as shown in Figures 7 and 8 for the tube and the drilled designs, respectively. The curvature change in the flow region near 0.25 *GPM (Re ≈ 3300) as* predicted by the model in Figure 7 is due to the transition of flow from laminar to turbulent.
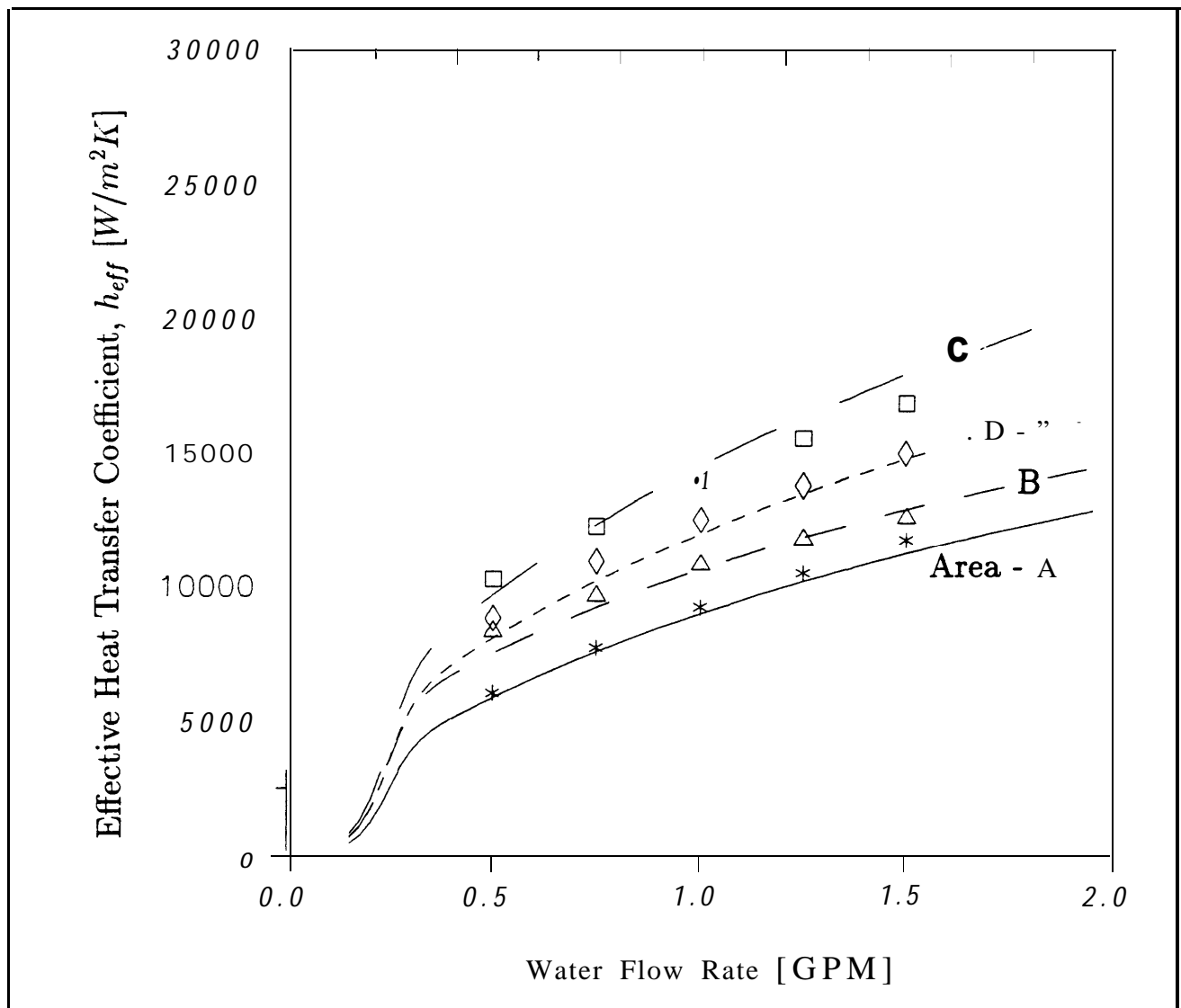
Figure 7: Comparison of Effective Heat Transfer Coefficient versus Water Flow Rate for Tube Design Cold Plate

v. SUMMARY

Two different design concepts for water-cooled cold plates have been presented. These concepts allow one to design water passages through a complex electronics packaging structure. Modeling and experiments were conducted to characterize the thermal and hydraulic performance of cold plate prototypes built using the two concepts. The hole design prototype showed high cooling capability, in terms of the heat transfer coefficient as defined in this paper, $7,000 < h_{eff} < 27,000$ W/m^2K for the water flow range of 0.5 to 1.5 GPM. The tube concept offers a lighter cold plate options with less manufacturing cost and slightly lower pressure drop. The measured heat transfer coefficients of the tube design prototype are between 6,000 to 17,000 W/m^2K for the same flow range.
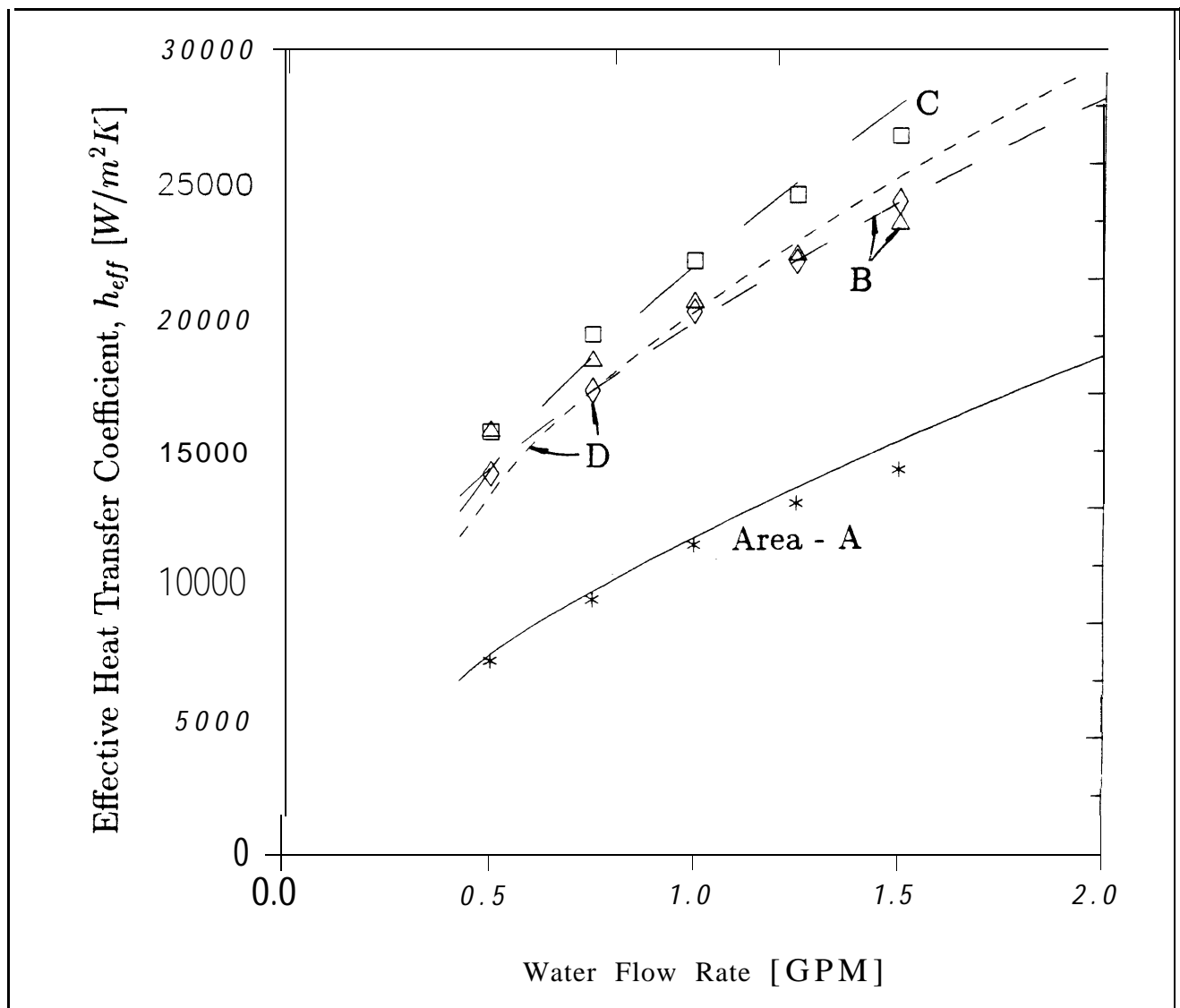
80

Figure 8: Comparison of Effective Heat Transfer Coefficient versus Water Flow Rate for Drilled Design Cold Plate

REFERENCES

[1] Churchill, S.W., 1977, "Comprehensive Correlating Equations for Heat, Mass and Momentum Transfer in Fully Developed Flow in Smooth Tubes", *Ind. Eng. Chem. Fundam.,* Vol. 16, No. 1, pp.109-1 16.

[2] Kakac, S., Shah, R.K., and Aung, W., 1987, *Handbook of Single-Phase Convective Heat Transfer,* John Wiley & Sons, New York.

[3] Idelchik, I.E., 1986, *Handbook of Hydraulic Resistance,* 2nd Ed., Chapter 6, Hemisphere Publishing Corporation, New York.

[4] A1-Arabi, M., 1982, 'Turbulent Heat Transfer in the Entrance Region of a Tube", *Heat Transfer Eng.,* Vol. *3,* pp. 76-83.

[5] Guyer, E. C., 1989, *Handbook of Applied Thermal Design,* Chapter 2, McGraw-Hill Book Co., New York.